# Charge Regulation Effects in Nanoparticle Self-Assembly

Tine Curk[1,*] and Erik Luijten[1,2,†]

[1]*Department of Materials Science & Engineering, Northwestern University, Evanston, Illinois 60208, USA*
[2]*Departments of Engineering Sciences & Applied Mathematics, Chemistry, and Physics & Astronomy, Northwestern University, Evanston, Illinois 60208, USA*

Nanoparticles in solution acquire charge through the dissociation or association of surface groups. Thus, a proper description of their electrostatic interactions requires the use of charge-regulating boundary conditions rather than the commonly employed constant-charge approximation. We implement a hybrid Monte Carlo/molecular dynamics scheme that dynamically adjusts the charges of individual surface groups of objects while evolving their trajectories. Charge regulation effects are shown to *qualitatively* change self-assembled structures due to global charge redistribution, stabilizing asymmetric constructs. We delineate under which conditions the conventional constant-charge approximation may be employed and clarify the interplay between charge regulation and dielectric polarization.

Most solvated materials and biomolecules acquire non-zero charge due to the dissociation or association of charged surface groups. For example, proteins, DNA, and silica nanoparticles attain their charge via proton dissociation [1,2]. The magnitude of the surface charge is determined by the solution conditions, such as pH, but also by the presence of other charged entities in the vicinity, via *charge regulation* (CR). Although this phenomenon has been theoretically studied since the seminal work by Kirkwood in the 1950s [3], the assumption that all objects carry a *constant* charge is still widely employed. This is especially striking since the surface charge distribution plays a key role in colloidal assembly and macromolecular structure formation, both in materials science [4] and in biomolecular systems, such as protein binding and condensation [1,5,6]. The situation is exacerbated by the fact that little is known about the many-body effects of CR on electrostatic aggregation.

Traditionally, the Poisson equation is solved using the constant-charge (CC) or the constant-potential (CP) boundary conditions. The CR boundary condition yields a solution that falls between these two limiting cases [7,8]. Charge regulation effects have been shown to change polyelectrolyte [9] and polymer brush [10,11] phase behavior and to enhance protein-protein interactions [1,6]. Poisson-Boltzmann theory has elucidated the strong dependence of surface charge on pH, but it is limited to the weak coupling regime and to static and simple geometries such as flat surfaces [2], a spherical particle [12], or a pair of particles [13,14].

Particle-based simulations avoid the approximations inherent to a mean-field approach. However, whereas molecular dynamics (MD) and Monte Carlo (MC) simulations of solvated systems with explicit charges are standard, acid-base dissociation is rarely taken into account. Notable exceptions include hybrid techniques for atomistic simulations in a constant-pH ensemble [15–17] and MC investigations of polyelectrolytes [18,19] or planar surfaces [20,21]. Computational cost has limited these studies to relatively small systems, so that many-body effects of CR have not been investigated, and its consequences for the self-assembly of charged objects are largely unknown.

Charge regulation is particularly relevant for aggregation owing to the relation between the charge distribution and the structure of the aggregate, which requires a self-consistent solution of the problem. Here, we assess the effects of CR by investigating a fully dynamic system of up to 100 objects with more than 30 000 explicit, dissociable sites. By implementing an efficient and parallelizable hybrid MD-MC scheme, we examine how aggregation and self-assembly are affected by CR. In addition, we combine our scheme with the Iterative Dielectric Solver (IDS) [22,23], a boundary-element method, to explore how dielectric polarization, another intrinsically many-body problem [24], affects CR.

We consider spherical particles with a fixed density of surface-attached dissociable groups. Each group, e.g., a weak acid, can be neutral or charged with a unit charge $q_0$. The probability $\alpha_i$ that a group $i$ is charged depends on the equilibrium constant $pK_i$ and the chemical potential of the dissociated ion $\mu$, but also on the local electrostatic potential $\psi(\mathbf{r}_i)$ at the position $\mathbf{r}_i$ of the group [7,8,18],

$$\frac{\alpha_i}{1-\alpha_i} = 10^{-pK_i} e^{-\beta\mu \pm \beta\psi(\mathbf{r}_i)q_0}, \tag{1}$$

where $\beta \equiv 1/(k_B T)$ is the inverse temperature and the $\pm$ applies to negatively (acid) and positively (base) charged

groups. Note that $\Delta pK_i = pK_i + \beta\mu \log_{10}(e)$ is independent of the choice of units. For acid dissociation in an aqueous solution, $\mu = -pH k_B T \ln(10)$. Equation (1) applies to every dissociable group in the system, so that the full set $\{\alpha_i\}$ determines the surface charge density $\sigma(\mathbf{r}) = \mp \sum_i \alpha_i q_0 \delta(\mathbf{r}_i - \mathbf{r})$. Thereby, these equations provide a self-consistent boundary condition for the Poisson equation, $\nabla \cdot [\varepsilon(\mathbf{r})\nabla\psi(\mathbf{r})] = -\sigma(\mathbf{r})$, with $\varepsilon(\mathbf{r})$ being the local permittivity.

We apply this scheme to objects immersed in a monovalent electrolyte, represented via the primitive model, with chemical potential pI [25]. Our hybrid MD-MC method works as follows: The system configuration evolves via conventional MD using the velocity-Verlet algorithm, with parameters and potentials described in the Supplemental Material [26]. After every $n_{MD}$ time steps, $n_{MC}$ MC steps are performed, where each step samples the charging state of a dissociable group, Eq. (1), or inserts/deletes salt ions. To obtain realistic dynamics, the relative frequency of the MD and MC steps should match the proper ratio between the particle diffusion and the dissociation rate. Here, however, we focus only on thermodynamic properties and equilibrium structures, so that the choice of $n_{MD}$ and $n_{MC}$ is guided by efficiency considerations. As both types of steps have the same computational complexity, an efficient convergence to equilibrium is obtained by setting $n_{MD} = n_{MC} = 1/\delta t$, with $\delta t$ being the MD time step.

Unlike the reaction ensemble method or the constant-pH ensemble method, which are restricted to a specific range of pH values and salt concentrations [18], this scheme consistently implements both salt ion insertion and solvent dissociation via $pK_s$ and is thus valid for any salt concentration or pH. In addition, within the primitive model we treat the dissociated charges and the monovalent salt ions as equivalent, which increases the performance of our MC scheme compared to existing implementations [28], cf. Supplemental Material.

We begin by exploring the influence of CR on a spherical particle covered with $n_{ss} = 792$ surface sites (Fig. 1, inset). To highlight effects of CR on the electrostatic interactions, we initially disregard polarization effects as well as London dispersion forces and evaluate the average charge $\langle q_L \rangle$ on this particle. Evidently, this charge depends on the dissociation constant and the solution conditions; in the Supplemental Material we examine pH dependence and provide a comparison to Debye-Hückel theory. Here, however, we are interested in a more subtle effect: How does the charge, and thereby the interactions, depend on the presence of other charged entities? We add a small particle with *constant* charge equal in magnitude to the charge on the isolated large particle, $q_s = -\langle q_L \rangle_{d\to\infty}$, and apply the metadynamics method [29] to calculate the potential of mean force (PMF) between the two particles, normalized by the magnitude of the Coulomb energy at contact $\lambda = q_s^2/[4\pi\varepsilon(R + r)]$ under CC conditions (Fig. 1).
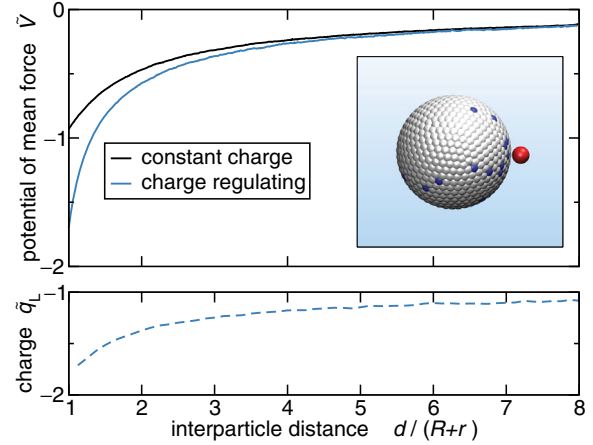


FIG. 1. Effect of charge regulation on pairwise interactions. Top: potential of mean force $V$ between a large particle with radius $R$ and a small particle (red sphere) with constant charge $q_s$ and radius $r$, normalized by the coupling strength $\lambda$ ($\tilde{V} = V/\lambda$). Charge regulation is realized through dissociable sites that can be either neutral or charged (white and blue, respectively, in the inset) and results in a significantly enhanced attraction (blue line) compared to a constant charge $q_L = -q_s$ on the large particle (black line). Bottom: corresponding (normalized) total charge on the larger particle, $\tilde{q}_L = q_L/q_s$ (dashed blue line). The parameters employed here correspond to a 6-nm silica particle in deionized water at pH = 7 [14]: $n_{ss} = 792$ ($\sigma_{ss} \approx 8$ nm$^{-2}$), $\Delta pK = -0.5$, $q_s = 12q_0$, $R = 4l_B$, $2r = l_B$, pI = 6.7, $\lambda = 32k_B T$.

Charge regulation results in a nearly twofold increase in the interaction strength at contact compared to the CC approximation. This arises due to the redistribution of charges on the sphere—an effect similar to the polarization of conducting objects—and due to the change in the total charge $q_L$ on the large particle, which depends on the proximity of the point charge $q_s$. In the absence of CR effects, an equivalent *conductive* sphere would yield an increase in the interaction strength by a factor of 1.6 [24]. At higher ionic strengths, the electrostatic interactions are screened and weakened. Crucially, however, in the presence of CR, the interaction at contact remains about twice as strong as the corresponding interaction under CC conditions, even at physiological salt concentration conditions (see Supplementary Material).

A central challenge in the rational design of materials is the prediction of structure. Our findings for a particle pair indicate that CR may significantly affect aggregation. Moreover, dielectric polarization has been shown to induce large-scale changes to self-assembled structures through local redistribution of charge *within* particles [24,30]. Since charge regulation allows *global* redistribution of charge, we may expect it to be an even more powerful factor. Thus, we turn to many-body effects and self-assembly of multiple particles. Binary mixtures of size-asymmetric particles give rise to a plethora of self-assembled structures [31,32]. We focus on a prototypical system of spherical particles with

size ratio 1:7, motivated by the observation that CR appreciably changes the pair interaction when a small particle is positioned at approximately $R/7$ from the surface, or at a center-to-center distance $d \approx 8R/7$ (Fig. 1).

To understand how CR can modulate the local arrangements of building blocks in a binary mixture, we start with a small system of three large and three small particles, at concentration $\rho = 0.0002R^{-3}$ and coupling strength $\lambda = 64k_{B}T$. We focus on charge-neutral systems to clearly decouple CR from other possible effects, such as the formation of extended structures due to nonzero net charge of the aggregate. In the conventional (CC) case, the particles form a compact, symmetric aggregate [Fig. 2(a)]. However, when the charge is no longer kept fixed and identical on each large particle, the CR simulation shows an extended conformation [Fig. 2(b)]. Interestingly, this is accompanied by symmetry breaking: The average net charge of the three large particles in Fig. 2(b) is $\bar{q}_{L} = \{9.8q_{0}, 22.3q_{0}, 16.0q_{0}\}$ for the top, middle, and bottom particles, respectively, indicating that CR stabilizes asymmetric, heterogeneously charged structures through a *global* redistribution of charge.

A similar symmetry-breaking transition has recently been reported for CR of membrane stacks [33]. A set of four large and four small particles shows the same trend, forming a symmetric (squarelike) structure under CC conditions [Fig. 2(c)], but an asymmetric structure under CR [Fig. 2(d)]. This charge redistribution due to CR
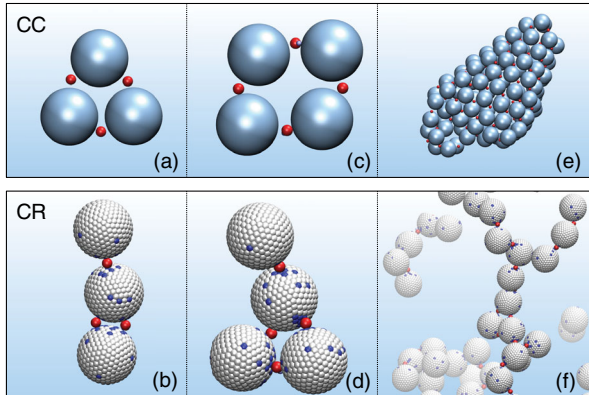


FIG. 2. Self-assembly of binary aggregates. Small particles (red) carry a constant charge $q_{s} = 16q_{0}$, while large particles either have a constant charge $q_{L} = -q_{s}$ [CC, blue spheres in panels (a), (c), and (e)] or are charge regulating [CR, spheres with neutral (white) or charged (blue) surface sites in panels (b), (d), and (f)]. In the CR case, $\Delta pK = -1.5$, which results in neutral structures, $\langle q_{L}\rangle \approx -q_{s}$. Whereas CC conditions give rise to compact structures, CR leads to anisotropic and open assemblies. This observation persists with increasing particle number: $N_{p} = 3, 4$, and 100 large and small particles in panels (a) and (b), (c) and (d), and (e) and (f), respectively, at ion concentration pI = 5.7. The CR images are instantaneous realizations; the charge distribution on the large particles is continuously fluctuating.

persists for larger systems and gives rise to much more extended structures than found in CC self-assembly. As noted, the CR-induced enhancement of pairwise interactions continues to hold at higher ionic strength. The same is true for the asymmetry imparted by CR (see Supplemental Material).

We illustrate this in a system of 100 large and 100 small particles at a concentration $\rho = 0.0043R^{-3}$ (lateral system size $L = 28.5R$). The structures are characterized by the local coordination number $z$, which measures the number of small particles within a distance $d_{n} = R + 3r$ (the first minimum of the radial distribution function) from each large particle. Under CR conditions, one-dimensional stringlike structures appear [$\langle z\rangle = 2.04$, Fig. 2(f)], compared to folded two-dimensional hexagonal packed monolayers with $\langle z\rangle = 2.80$ that form in the simulations employing CC conditions [Fig. 2(e)].

Arguably, open structures similar to Fig. 2(f) have been observed for conducting particles in a low-permittivity medium [30]. However, we emphasize that the underlying mechanism is different. In the case of dielectric mismatch, the total charge on each individual particle is conserved, and the polarization charge is redistributed across the surface of the particle; the conductivity of the particles then merely guarantees a constant potential on each surface. This differs from the CR process, where the CP limit would be realized by globally grounding all particles to a common potential, allowing free redistribution of charge among different objects and the solution. Such a system has, to our knowledge, not been investigated.

Of particular interest, then, is the question of the combined effects of CR and dielectric polarization. Like CR, polarization leads to charge redistribution and accompanying strong many-body effects [24]. Moreover, the prerequisite condition, namely a strong permittivity contrast between particles and the surrounding medium, occurs in numerous aqueous systems, including suspensions of silica or polystyrene colloids and protein solutions. To answer whether CR or polarization dominates, we augment our particle model with an additional boundary-element layer of 1472 patches uniformly distributed on each sphere, positioned just below the CR layer in the inset of Fig. 3. Dielectric polarization charges are controlled by the mismatch $\tilde{\varepsilon}$, which denotes the ratio of the dielectric constants of the particle and the surrounding solvent. After each MC and MD step, we employ the IDS to compute the induced charge on each surface element. Conversely, these polarization charges are taken into account when computing the dissociation probability of each surface group. We evaluate the role of dielectric effects by reexamining the system of Fig. 1 for two extreme cases: A small particle of fixed charge interacting with a large particle of either high permittivity (i.e., nearly conducting; $\tilde{\varepsilon} = 100$) or low permittivity ($\tilde{\varepsilon} = 0.01$). As is well known [30], for CC boundary conditions, the attraction between the large and
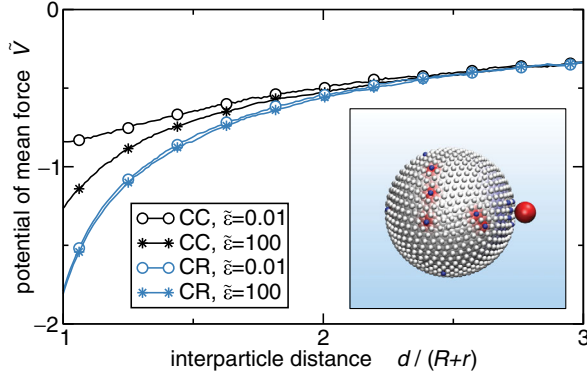
FIG. 3. Dielectric effects on the (normalized) potential of mean force $\tilde{V}$ for the particle pair described in Fig. 1, with the additional condition that the large particle is polarizable. Under constant-charge (CC) conditions, a particle with low dielectric constant ($\tilde{\varepsilon} = 0.01$) has a diminished attraction (open circles) and a high-dielectric particle ($\tilde{\varepsilon} = 100$) has an enhanced attraction (asterisks). Both cases are superseded by the attraction strength under charge-regulating (CR) conditions. Here, the high-permittivity case still is slightly stronger, but the effect is barely visible on the scale of the graph. The inset illustrates the CR-BEM model. The BEM layer of polarizable surface patches ($\tilde{\varepsilon} = 100$) is placed at a distance $R/8$ below the CR layer, with positive (red) or negative (blue) induced dielectric charges. The CR layer is shown as small white (neutral) or charged (blue) spheres.

the small particle is suppressed in the low-permittivity case and enhanced in the high-permittivity case (Fig. 3). Remarkably, however, CR almost completely screens any dielectric polarization charges, yielding a PMF that is nearly independent of $\tilde{\varepsilon}$ (cf. overlapping curves in Fig. 3). This observation is consistent with Kirkwood's explanation of the dielectric increment of protein solutions [3]. Charge regulation screens dielectric polarization; therefore, in the far field proteins can behave as high-dielectric objects even though the protein core has a dielectric constant significantly lower than water.

In view of the potentially far-reaching consequences of CR, it is an important question under which circumstances its effects can be ignored. Figure 3 illustrates that for a small particle with relatively high density of surface sites (a 6-nm silica particle in water), CR strongly affects the interactions. Conversely, we can estimate when the CC or CP approximation results in an error in the electrostatic interaction that is smaller than the thermal energy $k_B T$. We place a point charge $q$ at a distance $d$ from a charge-regulating surface with a mean surface charge density $\sigma$ and a maximum (fully ionized) charge density $\sigma_0$. In a mean-field approximation, $\alpha_i = \sigma/\sigma_0$, and the surface capacitance, determining the linear response of the surface charge, then follows from Eq. (1) as $C = \partial\sigma/\partial\psi = \sigma(1 - \sigma/\sigma_0)(-\beta q_0)$. In the absence of ionic screening, the change in the potential at the surface due to charge $q$ is $\Delta\psi = q/(4\pi\varepsilon d)$. The charge produced by the surface capacitance will be contained within
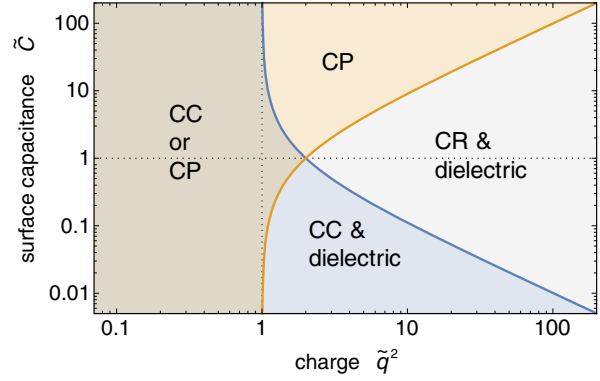


FIG. 4. Schematic diagram showing the applicability of the constant-charge (CC) and constant-potential (CP) approximations of CR. For sufficiently strong charges and intermediate values of the surface capacitance, the use of a full CR solver—as proposed in the main text—is required. In addition, in the two regions denoted by "dielectric," dielectric polarization effects can be important.

an area of size $\sim d^2$, since $d$ is the relevant length scale. The additional charge density due to CR is thus $\sigma_{CR} \sim -q\tilde{C}/[d^2(1 + \tilde{C})]$ [34], with the dimensionless capacitance $\tilde{C} \equiv -Cdl_B/(q_0^2\beta)$. We observe that the CC approximation is valid if the CR charge is sufficiently small, $-\sigma_{CR}qd \ll q_0^2/l_B$ or $\tilde{C} \ll 1/(\tilde{q}^2 - 1)$, where we define the reduced charge $\tilde{q} \equiv q/q_0\sqrt{l_B/d}$. Conversely, the CP limit implies an image charge $q_{im} \sim -q$, because for a single flat surface the global CP limit is equal to the local CP condition and can therefore be captured by a single image charge. The CP limit is justified when $(\sigma_{CR}d^2 - q_{im})q/d \ll q_0^2/l_B$ or $\tilde{C} \gg \tilde{q}^2 - 1$. The CP condition screens any possible dielectric polarization charges, and thus dielectric effects can be neglected. These two conditions can be parametrized by just two dimensionless variables, $\tilde{C}$ and $\tilde{q}$, allowing us to delineate the different regimes in Fig. 4.

This schematic also allows us to estimate the importance of CR for different particle sizes. Notably, the PMF in Fig. 3 was obtained for a particle of only a few Bjerrum lengths in diameter ($R = 4l_B$), corresponding to $\tilde{C} \sim 0.1$ and $\tilde{q}^2 \sim 200$. This condition indeed falls inside the CR region in Fig. 4. Note that the difference between high/low dielectric spheres in Fig. 3 is very small, but still larger than $k_B T$. Rescaling the (linear) system size $d \to \gamma d$ while keeping the Coulomb energy constant implies $q \to \gamma^{1/2}q$, and therefore, $\sigma \to \gamma^{-3/2}\sigma$. This rescaling keeps $\tilde{q}$ constant, but the surface capacitance $\tilde{C} \sim -\sigma dl_B/q_0$ changes as $\tilde{C} \to \gamma^{-1/2}\tilde{C}$ [35]. Thus, the CC approximation becomes increasingly more accurate as the particle size increases, which helps explain why the CC approximation works rather well for predicting experimentally observed crystal structures and clusters of micron-sized colloidal particles [31,32]. On the other hand, nanoscale particles

will generally exhibit very strong CR effects; e.g., our results [Fig. 2(b)] provide a possible explanation for the chain formation observed in nanoparticle assembly [36,37].

In summary, we have implemented a hybrid MD-MC technique for resolving CR effects in arbitrary dynamical systems. Utilizing this method, we have shown that CR-induced many-body effects can qualitatively alter the predicted self-assembled structures via the stabilization of asymmetrically charged aggregates. Both our numerical results and a scaling analysis demonstrate that CR is particularly important for charged objects that are a few Bjerrum lengths in size, such as proteins or nanoparticles, in which case CR screens dielectric polarization effects. Our method, as well as the general findings, is broadly applicable to macromolecular and colloidal systems [38].

Although we focused on acid/base dissociation, the method outlined in this Letter can be directly utilized to study the association or dissociation of arbitrary ionic groups. For example, the MC part of our approach, Eq. (1), is equivalent to existing adsorption models for studying calcium binding to proteins [41].

---

[*]curk@northwestern.edu

[†]luijten@northwestern.edu

[1] M. Lund and B. Jönsson, Charge regulation in biomolecular solution, Q. Rev. Biophys. **46**, 265 (2013).

[2] T. Markovich, D. Andelman, and R. Podgornik, Charge regulation: A generalized boundary condition? Europhys. Lett. **113**, 26004 (2016).

[3] J. G. Kirkwood and B. Y. Shumaker, The influence of dipole moment fluctuations on the dielectric increment of proteins in solution, Proc. Natl. Acad. Sci. U.S.A. **38**, 855 (1952).

[4] M. A. Boles, M. Engel, and D. V. Talapin, Self-assembly of colloidal nanocrystals: From intricate structures to functional materials, Chem. Rev. **116**, 11220 (2016).

[5] H.-X. Zhou and X. Pang, Electrostatic interactions in protein structure, folding, binding, and condensation, Chem. Rev. **118**, 1691 (2018).

[6] F. L. B. da Silva and B. Jönsson, Polyelectrolyte-protein complexation driven by charge regulation, Soft Matter **5**, 2862 (2009).

[7] B. W. Ninham and V. A. Parsegian, Electrostatic potential between surfaces bearing ionizable groups in ionic equilibrium with physiologic saline solution, J. Theor. Biol. **31**, 405 (1971).

[8] R. Podgornik, General theory of charge regulation and surface differential capacitance, J. Chem. Phys. **149**, 104701 (2018).

[9] E. Raphael and J.-F. Joanny, Annealed and quenched polyelectrolytes, Europhys. Lett. **13**, 623 (1990).

[10] P. Gong, J. Genzer, and I. Szleifer, Phase Behavior and Charge Regulation of Weak Polyelectrolyte Grafted Layers, Phys. Rev. Lett. **98**, 018302 (2007).

[11] M. Tagliazucchi, M. Olvera de la Cruz, and I. Szleifer, Self-organization of grafted polyelectrolyte layers via the coupling of chemical equilibrium and physical interactions, Proc. Natl. Acad. Sci. U.S.A. **107**, 5300 (2010).

[12] A. Bakhshandeh, D. Frydel, A. Diehl, and Y. Levin, Charge Regulation of Colloidal Particles: Theory and Simulations, Phys. Rev. Lett. **123**, 208004 (2019).

[13] I. Popa, P. Sinha, M. Finessi, P. Maroni, G. Papastavrou, and M. Borkovec, Importance of Charge Regulation in Attractive Double-Layer Forces Between Dissimilar Surfaces, Phys. Rev. Lett. **104**, 228301 (2010).

[14] G. Trefalt, S. H. Behrens, and M. Borkovec, Charge regulation in the electrical double layer: Ion adsorption and surface interactions, Langmuir **32**, 380 (2016).

[15] W. Chen, B. H. Morrow, C. Shi, and J. K. Shen, Recent development and application of constant pH molecular dynamics, Mol. Simul. **40**, 830 (2014).

[16] Y. Huang, W. Chen, J. A. Wallace, and J. Shen, All-atom continuous constant pH molecular dynamics with particle mesh Ewald and titratable water, J. Chem. Theory Comput. **12**, 5411 (2016).

[17] B. K. Radak, C. Chipot, D. Suh, S. Jo, W. Jiang, J. C. Phillips, K. Schulten, and B. Roux, Constant-pH molecular dynamics simulations for large biomolecular systems, J. Chem. Theory Comput. **13**, 5933 (2017).

[18] J. Landsgesell, L. Nová, O. Rud, F. Uhlík, D. Sean, P. Hebbeker, C. Holm, and P. Košovan, Simulations of ionization equilibria in weak polyelectrolyte solutions and gels, Soft Matter **15**, 1155 (2019).

[19] A. Murmiliuk, P. Kosovan, M. Janata, K. Prochazka, F. Uhlik, and M. Štěpánek, Local pH and effective p$K$ of a polyelectrolyte chain: Two names for one quantity? ACS Macro Lett. **7**, 1243 (2018).

[20] S. Madurga, C. Rey-Castro, I. Pastor, E. Vilaseca, C. David, J. L. Garcés, J. Puy, and F. Mas, A semi-grand canonical Monte Carlo simulation model for ion binding to ionizable surfaces: Proton binding of carboxylated latex particles as a case study, J. Chem. Phys. **135**, 184103 (2011).

[21] S. A. Barr and A. Z. Panagiotopoulos, Interactions between charged surfaces with ionizable sites, Langmuir **27**, 8761 (2011).

[22] K. Barros, D. Sinkovits, and E. Luijten, Efficient and accurate simulation of dynamic dielectric objects, J. Chem. Phys. **140**, 064903 (2014).

[23] H. Wu and E. Luijten, Accurate and efficient numerical simulation of dielectrically anisotropic particles, J. Chem. Phys. **149**, 134105 (2018).

[24] Z. Wang, Z. Gan, S. Jiang, Z. Xu, and E. Luijten, Anisotropic self-assembly of polarizable colloidal mixtures (2021).

[25] All concentration-based quantities, e.g., pI, are expressed in units of $l_B^{-3}$, with the Bjerrum length $l_B = \beta q_0^2/(4\pi\varepsilon)$.

[26] See Supplemental Material at http://link.aps.org/supplemental/10.1103/PhysRevLett.126.138003 for calculation details and supporting data, which includes Ref. [27].

[27] D. J. Wales and S. Ulker, Structure and dynamics of spherical crystals characterized for the Thomson problem, Phys. Rev. B **74**, 212101 (2006).

[28] J. Landsgesell, P. Hebbeker, O. Rud, R. Lunkad, P. Košovan, and C. Holm, Grand-reaction method for simulations of ionization equilibria coupled to ion partitioning, Macromolecules **53**, 3007 (2020).

[29] G. Fiorin, M. L. Klein, and J. Hénin, Using collective variables to drive molecular dynamics simulations, Mol. Phys. **111**, 3345 (2013).

[30] K. Barros and E. Luijten, Dielectric Effects in the Self-Assembly of Binary Colloidal Aggregates, Phys. Rev. Lett. **113**, 017801 (2014).

[31] M. E. Leunissen, C. G. Christova, A.-P. Hynninen, C. P. Royall, A. I. Campbell, A. Imhof, M. Dijkstra, R. van Roij, and A. van Blaaderen, Ionic colloidal crystals of oppositely charged particles, Nature (London) **437**, 235 (2005).

[32] A. F. Demirörs, J. C. P. Stiefelhagen, T. Vissers, F. Smallenburg, M. Dijkstra, A. Imhof, and A. van Blaaderen, Long-Ranged Oppositely Charged Interactions for Designing New Types of Colloidal Clusters, Phys. Rev. X **5**, 021012 (2015).

[33] A. Majee, M. Bier, R. Blossey, and R. Podgornik, Charge regulation radically modifies electrostatics in membrane stacks, Phys. Rev. E **100**, 050601(R) (2019).

[34] The total potential change $\Delta\psi$ at the surface will be approximately $\beta\Delta\psi q_0^2/l_B \sim q/d + \sigma_{CR}d$.

[35] Assuming low occupancy of surface sites, $\alpha \to 0$, which is expected for sufficiently large particles.

[36] Z. Tang, N. A. Kotov, and M. Giersig, Spontaneous organization of single CdTe nanoparticles into luminescent nanowires, Science **297**, 237 (2002).

[37] X. Zhang, L. Lv, L. Ji, G. Guo, L. Liu, D. Han, B. Wang, Y. Tu, J. Hu, D. Yang, and A. Dong, Self-assembly of one-dimensional nanocrystal superlattice chains mediated by molecular clusters, J. Am. Chem. Soc. **138**, 3290 (2016).

[38] An open-source implementation in the LAMMPS MD package [39] is in preparation [40].

[39] S. J. Plimpton, Fast parallel algorithms for short-range molecular dynamics, J. Comp. Phys. **117**, 1 (1995).

[40] T. Curk, J. Yuan, and E. Luijten (to be published).

[41] F. Roosen-Runge, F. Zhang, F. Schreiber, and R. Roth, Ion-activated attractive patches as a mechanism for controlled protein interactions, Sci. Rep. **4**, 7016 (2014).